

**Leszek CHMIELEWSKI**

Institute of Fundamental Technological Research, PAS, Warsaw  
lchmiel@ippt.gov.pl

## **THE AH LINE EDGE DETECTOR AND THE HIERARCHICAL HOUGH TRANSFORM AS DETECTORS OF THE IRRADIATION FIELD IN SIMULATION IMAGES<sup>1)</sup>**

### **Abstract**

The necessity of solving a practical problem in the analysis of medical images has become the occasion to propose new image processing solutions. The problem is related to the quality assessment in the oncological radiotherapy with external beams. The algorithm of finding the families of lines which define the dimensions and the coordinate system of the irradiation field is proposed. It comprises a new line edge detector, a robust Hough transform-based algorithm for finding lines and a generator of hypotheses on the sought description of the irradiation field. The proposed *AH line edge detector* is local, fast, easy to implement in parallel, has practically no parameters and yields narrow lines. If the analysed image, related to radiotherapy planning, contains too little information, the user is supported in providing additional data manually.

**keywords:** *line edge detector, irradiation field detection, hierarchical Hough transform, radiotherapy, quality assessment.*

## **1 INTRODUCTION**

In the radiotherapy of cancer, the quality of reproduction and repeatability of the planned geometry of the irradiation process is performed by comparing the planned geometry, recorded in the *simulation image* (Fig. 1a, b), with the realized geometry, recorded in a series of *portal images*, one for each irradiation session. The comparison is difficult due to that the quality of the portal image is inevitably low, and various geometrical distortions between the images are present, besides the differences which should be measured. In the majority of the existing software tools supporting such an assessment, either manual registration of the images is used, or the corresponding points of the images must be known, and these not always can be found automatically. The whole procedure of mostly automatic measurement of the quality of a given radiotherapy session has been described in [6, 10] and implemented in the program *AutoPort*. There still exists a need of automatising more elements of this procedure, which is attempted in this paper.

---

<sup>1</sup> K. Wojciechowski, editor. *Proc. Int. Conf. Computer Vision and Graphics ICCVG 2002*, vol. 1, pages 192–199, Zakopane, Poland, Sept 25-29, 2002.

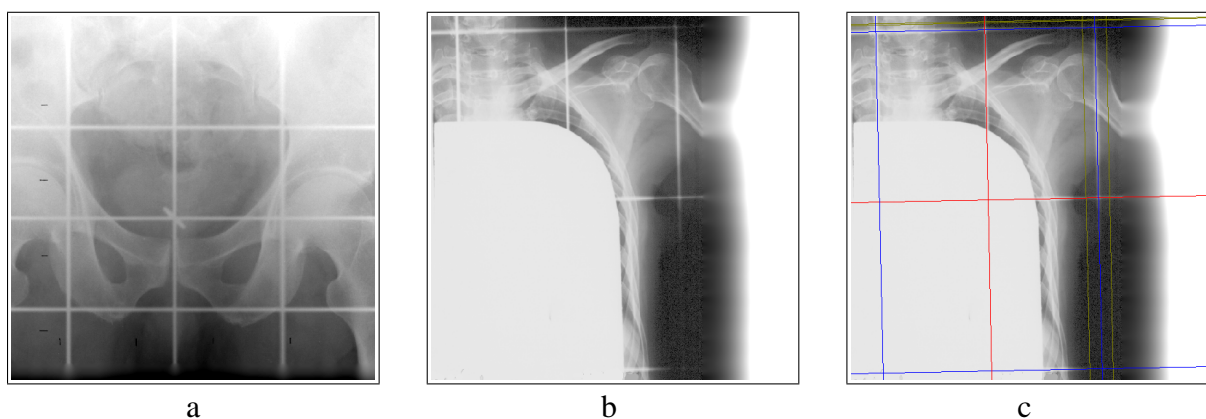


**Fig. 1.** Edges and coordinate system of the irradiation field in the simulation images, marked with wires. a: pelvis, all lines visible; b: breast, some lines visible only in small fragments; c: example of field description result: image (b) with field lines found and interpreted as field coordinate axes – red and edges – blue (yellow lines are those detected but not used in the description).

The literature on the analysis and registration of the simulation and portal images is broad and mainly the problem of image registration is considered. Here let us cite [8] where the rectilinearity of field edges was utilised in the detection process, and the Radon transform, closely related to the Hough transform, was applied. The systems in which only the manual indication of the features in the analysed images is possible are still in use [1].

In the simulation image, the irradiation field is marked with wires positioned by the operator during the simulation process. The images of these wires normally form a very regular pattern: three, usually vertical, lines and three lines perpendicular to them. The central lines represent the coordinate system of the irradiation field; the lateral lines – the field edges (Fig. 1c).

The regularity of the layout of the considered lines should make it possible to automatise the process of detecting the irradiation field, even in cases when some of the line fragments are missing in the image. This would be useful especially if manual marking of the important elements of the description of the irradiation field were difficult, as in the example of Fig. 1b, c, where the field centre can not be seen directly. The regularity of the images to be analysed creates a possibility of designing a very robust algorithm, highly insensitive to possible errors and omissions in the data derived from the images.

The proposed algorithm has three elements. First, the *line edges* (called also *ridge edges*) present in the simulation image are detected with a novel detector, called the AH detector, described in Section 2. Then, the families of lines are found with the version of the Hough transform, in which the regularities of the analysed image are utilised to make the process more robust. This is described in Section 3. In Section 4 the last stage of the analysis is described, where a set of hypotheses on the irradiation field description – interpretation of lines as the field edges and coordinate axes – is formed. If none of the hypotheses is correct, as in the case of the images which contain too little data (Fig. 2a), the additional information should be entered by the user to finalise the calculations, as shown in Section 5. Some theoretical considerations related to the structure of the proposed AH detector are outlined in Section 6.

## 2 DETECTION OF LINE EDGES

In the author's opinion, line edge or *ridge edge* detectors receive small interest. In the image processing handbooks, like [9, 14], the Canny line edge detector [2] and its variants (e.g. [3]) remain the standard. Such new ideas as the competitive edge detector [4], which could lead to the invention of original roof or line edge detectors, came to a failure [5]. The necessity of optimising the mask contents in the Canny detector for the widths of lines expected in the image was an incentive to look for a detector without, or nearly without the scale effects. Nevertheless, the Canny criteria of a good detector were paid much attention.

The name ‘‘AH detector’’ will be used for the proposed line edge detector<sup>1</sup>. The algorithm will be described first, and then the rationale for its design will be presented.

1. In each pixel, four one-dimensional windows with centres located in this pixel are formed, in angular intervals of 45°. For each pixel, each window, separately, the steps 2-4 are performed. Step 5 concludes the processing for each pixel.
2. Trigger: if the central pixel of the window is the maximum for this window, then go to 3, else set the result to zero and go to step 5 immediately.
3. Growth: Calculate growth measures  $G_l, G_r$ , starting from left and right window ends, respectively, to its centre. Let  $I(x)$  be the intensity in the window, and  $x = x_l$  at the left end of window,  $x = x_c$  at its centre and  $x = x_r$  at the right end. Only positive increments of intensity are taken into account:

$$G_l = \sum_{x=x_l}^{x_c-1} \max\{[I(x+1) - I(x)], 0\}, \text{ and symmetrically} \quad (1)$$

$$G_r = \sum_{x=x_c+1}^{x_r} \max\{[I(x-1) - I(x)], 0\}. \quad (2)$$

4. Result: take the smaller growth measure for the considered window. To receive the final result, multiply it by the measure of symmetry  $s$  in the window:

$$R = \max[s \min(G_l, G_r), 0], \text{ where} \quad (3)$$

$$s = 1 - |G_l - G_r| / (G_l + G_r). \quad (4)$$

5. As the final result for each pixel, the maximum of results for its windows is taken. The output is a real value. After processing the whole image, the output is scaled into the range of possible integer pixel values.

**Lines are relatively straight and distant from each other – step 1** One-dimensional masks used cater for effectiveness. Separate analysis of masks make this purely local algorithm easy to parallelise. Results weakly depend on mask length, which can be e.g. 7-15 pixels.

**One pixel-wide results expected – step 2** This step works for well localised response, and effectiveness.

**Edge is a steep ridge – step 4** The good line edge is a relatively symmetrical ridge, with steep slopes on *both* sides. Step edges have only one slope and should not be detected.

**Edgel direction found – step 5** This profitable side-effect of the algorithm can be utilised if the information on which particular window gave the largest output is stored.

An example of results from the proposed AH detector is shown in Fig. 5, compared with the result from a 1D Canny detector optimised for 7 pixel-wide edges applied instead of the above steps 2-4. The comparison reveals the following features of the AH detector:

- edges found are very narrow – 1 to 2 pixels – and have good contrast;
- response for step edges is much smaller than that for the line edges;
- detector is more sensitive to isolated peak noise than the Canny detector.

The first two of the features are virtues, and the last one is a drawback, which can not be overcome as long as the local nature of the detector is to be maintained. Some more considerations on the design of the detector can be found in Section 6.

---

<sup>1</sup> AH stands for *ad hoc*. Actually the detector was invented, implemented and tested in one day, without the theoretical analysis which came later. Unexpectedly, it appeared not very fruitful, as described in Section 6.

### 3 DETECTION OF THE FAMILIES OF STRAIGHT LINES

For finding the locations of long straight lines, the Hough transform is the optimal tool [11, 12]. In the case of perpendicular families of lines, the hierarchical approach slightly similar to that used in [13] can be used. The radius-angle straight line representation is used [7]:  $x \cos(\varphi) + y \sin(\varphi) = r$ .

First, the Hough transform of the whole image is found, with coarse angle and radius accumulator cell dimensions, for example, 1 angular degree and 1 pixel. Let us denote it by

$$H(r, \varphi) : (r, \varphi) \rightarrow N^2, \quad r \in \langle 0, r_{\max} \rangle \times N, \quad \varphi \in \langle 0, 360 \rangle \times N. \quad (5)$$

Then, the transform space is folded so that all quadrants fall into the angle range of the first quadrant, and the maximum counts for radii are summed for the four quadrants<sup>2</sup>:

$$H_f(\varphi) = \sum_{i=0}^3 \max_r [H(r, \varphi + i * 90^\circ)], \quad \varphi \in \langle 0^\circ, 90^\circ \rangle \times N. \quad (6)$$

In this way, the information on the dominating angle of all the straight lines forming the perpendicular families is gathered from all the image data. The maximum of  $H_f(\varphi)$  indicates this angle –  $\varphi_{max}$  – with the accuracy not worse than  $\pm 1^\circ$ . To find the straight lines in the image, it is enough now to perform the second-level Hough transforms, one for each quadrant<sup>2</sup>, with high angular and radial accuracy, for example, 0.2 angular degree and 0.2 pixel, in the angular ranges  $\langle \varphi_{max} + i * 90^\circ - 1, \varphi_{max} + i * 90^\circ + 1 \rangle$ ,  $i = 0, \dots, 3$ .

### 4 FORMING THE HYPOTHESES ON THE FIELD DESCRIPTION

The detected lines are sorted in each perpendicular family, according to the intensity of the peaks in the second-level Hough transform related to them, considered as their *quality*. Starting from the lines with the best quality, a predefined number (e.g. 16) of hypotheses on the six-tuples of lines, three in each family, are formed. Each hypothesis contains two central and four lateral lines, representing the axes of the coordinate system, and the edges of the irradiation field visible in the analysed simulation image. First, in each family the hypotheses are formed separately, by taking triplets of the lines, with gradually decreasing quality, in all possible combinations. Then, in each family the formed triplets are sorted according to the criterion in which the symmetry measure – distance of the inner line from the middle between the two outer ones – is multiplied by the smallest of the qualities of the three lines. Finally, the best triplets, in all possible combinations, are used to form the hypotheses. The process is stopped when the predefined number of hypotheses is found.

The hypotheses formed are presented to the user in a graphical way, and can be switched between with a slider. In the majority of cases the first hypothesis is the right one.

For a typical  $500 * 500$  pixel image, like those in Fig. 1 or 2a, the whole analysis takes less than two seconds on a 1000 MHz Pentium III processor. This comprises around 0.8 s for line detection, 0.7 s for the Hough transforms and less than 0.1 s for the hypothesis formation.

### 5 THE DIFFICULT CASES: USER INTERVENTIONS

In the clinical practice such ‘difficult’ images as that in Fig. 2a are often encountered. Some of the lines can be hardly visible due to low quality of the scanned image, or because of occlusion by the images of the shields introduced during the therapy planning. The fully automatic analysis can not cope with such images, as the important data are missing. Nevertheless, some of the elements describing the irradiation field are still detectable. The result the software presents is incomplete then – some of the detected lines are faulty and none of the formed hypotheses is acceptable (Fig. 2c).

<sup>2</sup> Usually the image occupies the first quadrant. Then, the angles in the third quadrant relate to “impossible” lines and can be omitted in the whole analysis.

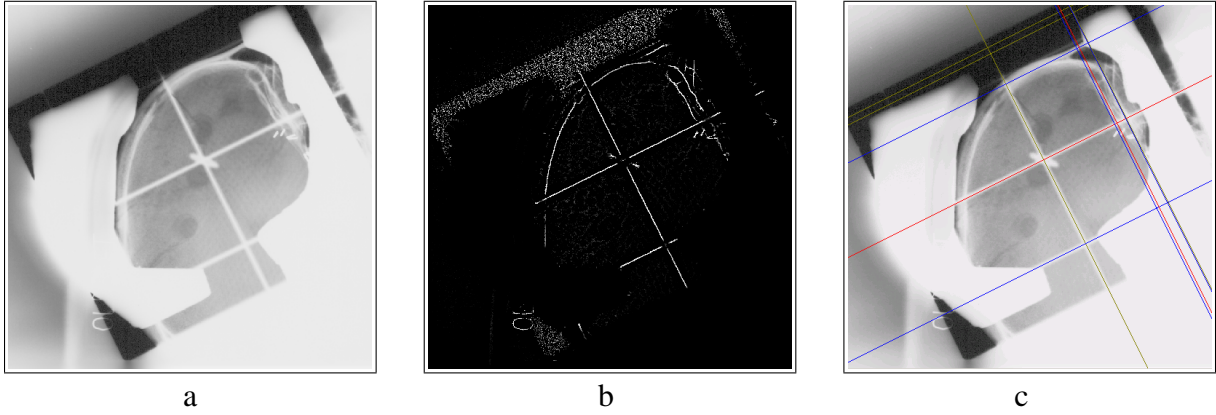


**Fig. 2.** Example of a difficult image. a: source; b: detected edges – some necessary line edges are missing; c: not all the lines were found and hypotheses on the field data are improperly formed.

In such cases, the program `AutoPort` makes it possible to choose not the whole hypotheses, but the single lines from those found, and to complement them manually with the missing characteristic points. Even if no lines are found, the user can indicate a set of points which describe the field edges and central lines.

To define the irradiation field, it is necessary to show the coordinate centre, the direction of one of the axes, and the field edges in the horizontal and vertical direction. The more lines found automatically are correct, the less lines or points the user must show. For example, if all but one lateral line is correctly detected, and the field is symmetrical, it is enough to state that the missing line should lie oppositely to the detected lateral one, on the other side of the central line. If at least one line is known, then the direction of all the edges is known precisely. If no lines are found, the direction can be determined by indicating the coordinate origin and one more point on one of the axes.

Nine cases of definition of the coordinate system and eight cases for each pair of lateral lines have been described and implemented in `AutoPort`. This gives 576 ways of defining the irradiation field. To make it easier for the user to know whether the definition is incomplete, complete, or there is an overdefinition, the software shows clear graphical signs. In case of the overdefinition, the surplus elements recommended for deletion, with the primary and secondary priority, are also indicated. In Fig. 3a the “manual” tab of the irradiation field description panel is shown, with the overdefinition marked with the red dashed line. Such a panel appears near the image in which the selections are made, like that in Fig. 2c. As soon as the user unselects the recommended items, the next items for deletion appear, if any. Finally, the green mark of the completeness of the field definition appears (Fig. 3b).

## 6 THEORETICAL CONSIDERATIONS ON THE AH LINE EDGE DETECTOR

Here some simple but appealing theoretical considerations will be mentioned, which could lead to different designs of the proposed AH line edge detector.

**Growth measure** A good edge is thin, so a twice thicker line should yield twice weaker output. Such an effect would be received if instead of Eqs. (1,2,3), the following are used

$$G_l = \sum_{x=x_l}^{x_c-1} [I(x+1) - I(x)] / (2|x - x_c| - 1), \quad (7)$$

$$G_r = \sum_{x=x_c+1}^{x_r} [I(x-1) - I(x)] / (2|x - x_c| - 1), \quad (8)$$

$$R = \max[s \max(G_l, G_r), 0], \quad (9)$$

with  $s$  as defined in (4). Functions (7,8) have the desirable property of disappearing far from the mask centre. However, simple calculations indicate that for lines with uniform brightness, the output would also be flat, without the maximum in the middle of the line (Fig. 4a, b, d).

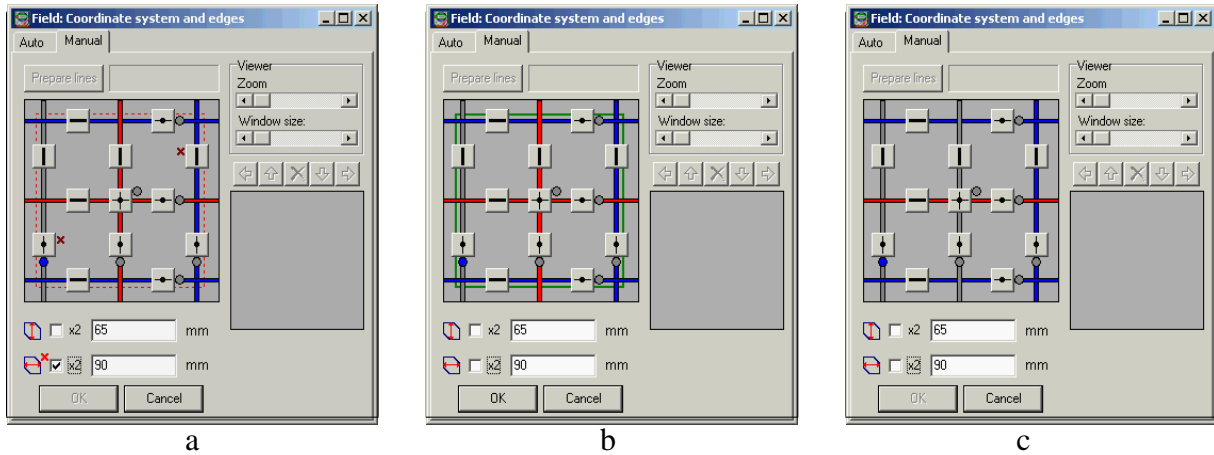


**Fig. 3.** The “manual” tab of the field description panel for a difficult image, like in Fig. 2. a: over-definition, marked with red dashed line; primary recommendation to unselect the “show half field” checkbox (red cross), secondary – point on the left or line on the right (brown crosses); b: complete definition received from (a), marked with green line; c: incomplete definition after further unselecting the central vertical line.

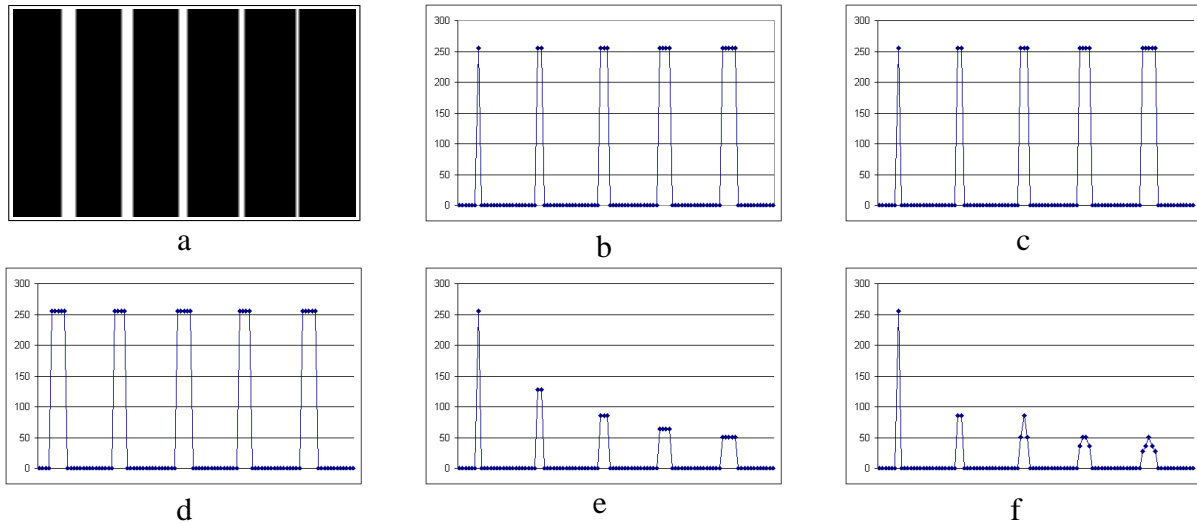


**Fig. 4.** Results of line edge detection for a test image with lines of different widths; a: image; b-d: horizontal cross-sections of intensity functions. a, b: test data; c: AH detector as described in Section 2; d: Canny line edge detector optimised for 7 pixel-wide edges, for comparison; e: AH detector with output inversely proportional to the line width, Eqs. (7,8,9); f: detector as in (e), tailored to yield thin edges, Eqs. (7,8,10).

**Symmetry measure and result** If Eqs. (7,8) are used with the result simplified from (9,4) to

$$R = \min(G_l, G_r), \quad (10)$$

then flat edges give a maximum in the middle, and step edges give zero output, as desired. However, the property of having the edge intensity strictly inversely proportional to edge width holds only for edges with odd width (Fig. 4f). Even width edges have output as that of the closest larger odd one.

Unexpectedly, although the detector designs according to the Eqs. (7,8) and (9) or (10) give nicer results on test images than the proposed AH detector (Fig. 4c), they give apparently worse results on real-life images used in our analyses (Fig. 5d, e), mainly due to worse behaviour for noisy images. Therefore, the version described in Section 2 can be considered as the final version of the AH detector.

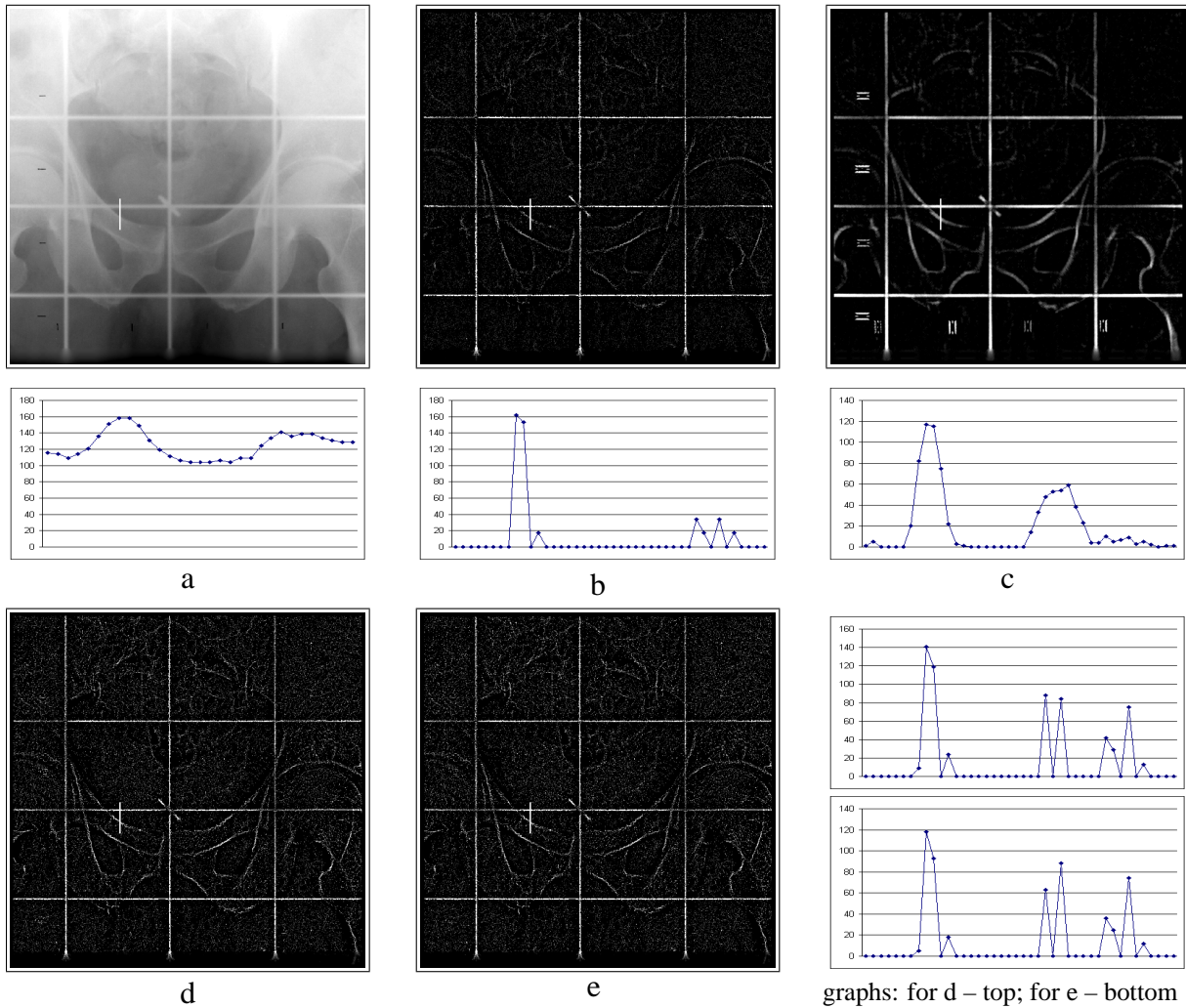


**Fig. 5.** Comparison of results of edge detectors. a: source image (Fig. 1a) and intensity profile on a line marked white, downwards; b: output of the AH detector and its intensity profile on the same line; c: output of the Canny line edge detector; d: AH detector with output inversely proportional to the line width, Eqs. (7,8,9); e: detector as in (d), tailored to yield thin edges, Eqs. (7,8,10).

## 7 CONCLUSION

In the simulation image made to plan the geometry of the radiation therapy, the lines which represent the edges and the coordinate system of the irradiation field are visible. To detect and interpret these lines, a set of algorithms have been designed.

The pixels of the line edges (or *ridge edges*) are successfully detected with the AH line edge detector, designed specially for the considered task. The detector behaves very desirably in spite of its simple structure, although more studies are necessary to explain why the developments derived from some theoretical analysis unexpectedly decrease the quality of the detection results.

The found edge pixels are grouped into the straight lines with the use of the hierarchical Hough transform. The set of hypotheses on the representation of the irradiation field, founded upon the lines formed, is put forward. The user selects the best of them, which is usually the first one. If neither of the hypotheses is correct, the set of detected lines is incomplete or no lines can be found at all, the user can manually indicate the locations of the characteristic features of the field – lines or points. The software supports the user in forming the consistent description of the field, in any of the numerous ways in which the irradiation field can be described with the characteristic lines and points.

The proposed algorithms form a very robust tool together. It makes it possible to efficiently analyse

also such images in which the manual indication of the characteristics of the considered irradiation field would be very difficult or impossible, due to the absence of features directly representing these characteristics in the image. The examples of such a situation could be a case when the irradiation field center is occluded by the shield, or a case when some of the lines is visible only in its short fragment.

The described processes are a part of the larger process of assessing the quality of the radiation therapy of cancer, with the use of the simulation and portal images. The whole quality assessment process is supported with the program AutoPort, the fragments of which have been described in this paper. The program has been developed in cooperation with the Holycross Cancer Centre in Kielce and is used there in everyday clinical practice.

**Acknowledgement** The presented work was partly supported by the Committee for Scientific Research, Poland, under the grant no. KBN 4 P05B 064 18.

## REFERENCES

- [1] J. Cai, J. C. H. Chu, A. Saxena, L. H. Lanzl. A simple algorithm for planar image registration in radiation therapy. *Med. Phys.*, 25(6):824–829, 1998.
- [2] J. Canny. A computational approach to edge detection. *IEEE Trans. PAMI*, 8(6):679–698, 1986.
- [3] S. Castan, J. Zhao, J. Shen. Optimal filter for edge detection. In *Proc. 1st European Conf. Computer Vision*, pages 13–17, Antibes, France, Apr 1990.
- [4] L. Chmielewski. The concept of a competitive step and roof edge detector. *Machine Graphics & Vision*, 5(1-2):147–156, 1996.
- [5] L. Chmielewski. Failure of the 2D version of the step and roof edge detector derived from a competitive filter. Report of the Division of Optical and Computer Methods in Mechanics, IFTR PAS, Dec 1997.
- [6] L. Chmielewski, P. Gut, P. Kukołowicz, A. Dąbrowski. Robust matching of images by an algorithm based on voting for treatment accuracy assessment in radiotherapy. In M. Kurzyński, E. Puchała, M. Woźniak, editors, *Proc. 2nd Polish Conference on Computer Pattern Recognition Systems KO-SYR 2001*, pages 211–216, Miłków, Poland, May 28-31, 2001. Wrocław University of Technology. Available also at: <http://www.ippt.gov.pl/~lchmiel>.
- [7] R. D. Duda, P. E. Hart. Use of the Hough transform to detect lines and curves in pictures. *Comm. Assoc. of Computing Machinery*, 15:11–15, 1972.
- [8] K. Eilertsen, A. Skretting, T. L. Tennvassas. Methods for fully automated verification of patient set-up in external beam radiotherapy with polygon shaped fields. *Phys. Med. Biol.*, 39:993–1012, 1994.
- [9] R. C. Gonzalez, R. E. Woods. *Digital Image Processing*. Addison-Wesley, Reading, MA, 1992.
- [10] P. Gut, L. Chmielewski, P. Kukołowicz, A. Dąbrowski. Edge-based robust image registration for incomplete and partly erroneous data. In W. Skarbek, editor, *Proc. 9th Int. Conf. CAIP 2001*, volume 2124 of *LNCS*, pages 309–316, Warsaw, Poland, Sept 5-8, 2001. Springer Verlag.
- [11] P. V. C. Hough. A method and means for recognizing complex patterns. U. S. Patent 3.069.654, 1962.
- [12] J. Illingworth, J. Kittler. A survey of the Hough transform. *Comp. Vision, Graph., and Image Proc.*, 44(1):87–116, 1988.
- [13] J. Princen, J. Illingworth, J. Kittler. A hierarchical approach to line extraction based on the Hough transform. *Comp. Vision, Graph., and Image Proc.*, 52(1):57–77, Oct 1990.
- [14] M. Sonka, V. Hlavac, R. Boyle. *Image Processing, Analysis and Machine Vision*. Brooks/Cole Publishing, 2nd edition, 1999.